acp-2016-886: Thermodynamic and dynamic responses of the hydrological cycle to solar dimming

Reviewer Comments are written in black font, and the Author Responses are in blue.

Response to RC1

General comments:

1. I would periodically get lost in the paper and had to re-read quite a number of lines. It would help if there were an outline at the beginning (maybe even a numbered list) of the factors that affect hydrological cycle changes. Then you can go through them one by one.

Thank you for the suggestion. At the end of the Introduction (Section 1), we have added a bulleted list of the factors we investigate in subsequent sections. We also added opening sentences to Sections 2.1, 2.2., and 2.3 to reorient the reader.

2. The abstract doesn't really say much, and the conclusions don't appear to agree with the results presented. Maybe I'm confused somewhere, in which case I think the description needs to be clearer.

We have revised the abstract to better summarize the results. Thank you for the advice.

Specific comments:

Page 1, line 24: Not all of the models were run for 500 years after spin-up. This really varies among the different modeling groups.

We have deleted this sentence, as the protocol for the GeoMIP experiments is addressed in Kravitz et al. 2010, which we cite.

Page 2, line 8: Why only 12? You should say more about this here.

We now explain this in the text.

Page 2, lines 24ff: This isn't a sentence.

The sentence is no longer interrupted by Equation (1) and reads more clearly now.

Page 3, lines 1ff: Somewhere in here, you should discuss how well these assumptions hold, and if they don't, what you can still learn.

We have added discussion of these assumptions, which better frames the subsequent adaptation of Byrne and O'Gorman's "extended scaling," which accounts for the fact that an assumption of constant relative humidity breaks down over land.

Page 3, line 6: Instead of "project", use "study" or something like that.

This has been changed.

Page 4, lines 1-2: I don't think this is quite fair. They had a lot of warming at high latitudes in particular, so it makes sense there would be a P-E responds, regardless of whether the temperature response to 4xCO2 is compensated.

We agree that it is unsurprising that the thermodynamic scaling calculation shows a P-E increase at high latitudes in BNU-ESM, due to the particularly large positive G1-Preindustrial temperature anomalies in this model (Fig. 4B). We have clarified these sentences.

Page 5, line 22: Typo - two periods at the end of the sentence.

This is now corrected.

Page 6, lines 14 and 16: Citation is coming out weirdly. Put 2014 on line 14.

Thank you. We have corrected this.

Page 7, line 21: This doesn't strike me as consistent with what you discussed earlier, nor is it what figure 4 shows.

Thank you for drawing attention to this. We have changed the paragraph to convey the relative importance of the three mechanisms we assessed in the study. The main driver of P-E changes under solar dimming is the Hadley circulation.

Page 8, lines 6-7: This is not correct as written. Turning down the sun by a uniform fraction cannot restore preindustrial P–E patterns. That doesn't say anything about geoengineering as a whole.

We have revised the end of this paragraph to reflect this distinction.

Figure 7: The paper by Haywood et al., 2015, GRL might be relevant here. (You don't need to do anything about this unless you want to – I just thought you'd find it interesting.)

Thank you for the suggestion, as the work of Haywood et al. is indeed relevant. We have now cited 2 papers by Haywood et al. (2013, Nature Climate Change; and 2016, GRL) in the fourth to last paragraph of Section 2.3.

Response to RC2

I recommend this paper be rejected. It presents little new information. It repeats results from previous papers. And it ignores the seasonal cycle in precipitation and evaporation which includes a lot of physics and monsoon responses, as analyzed by Tilmes et al. (2013). The conclusions are either obvious or not sufficiently diagnosed to add to understanding.

We disagree with your assessment of the paper. No previous study has decomposed the hydrological response to geoengineering into thermodynamic, relative humidity-driven, and dynamical components. In fact, no previous study has plotted the Hadley streamfunction

changes in the G1 experiment, and this was identified as a valuable future research direction by Kravitz et al. 2013c, as noted in our Introduction. Thermodynamic scaling captures the general spatial structure of P-E changes under global warming, as discussed in Held and Soden (2006), but we find that it is less explanatory of the hydrological response to geoengineering. Relative humidity changes over land are substantial in GeoMIP simulations of solar dimming, though our use of an extended thermodynamic scaling, after Byrne and O'Gorman (2015), demonstrates that local relative humidity changes play a relatively small role in the zonal mean hydrological cycle (Fig. 4). Our study reports, for the first time, that changes in tropical atmospheric dynamics dominate the P-E response to uniform solar dimming, and that these tropical rainfall shifts may be related to the interhemispheric contrast in the temperature response. This implies that the factors responsible for variations in the interhemispheric temperature response among models could ultimately explain the direction of the annual mean shift of the Intertropical Convergence Zone. This analysis is novel, and the conclusions cannot be dismissed as obvious.

In the interest of presenting a self-contained and cohesive paper, we decided to include the ensemble mean temperature change between G1 and the Preindustrial (Fig. 1), the ensemble mean P-E anomaly (G1-Preindustrial) (Fig. 2), and the ensemble mean P and E anomalies separately (Fig. 3). We now repeat our citation of Kravitz et al. 2013a where these figures appear in the manuscript to emphasize that these are not new results. These figures are included for clarity of presentation and to provide crucial context for the subsequent seven figures of novel analysis on which the paper focuses.

We greatly appreciate your comment on the importance of the seasonal cycle, as this motivated further analysis that led to additional new results. We have added the July-August-September and January-February-March streamfunction anomalies for G1-piControl (Figures 7 and 8), as well as the correlations of the ITCZ shifts with the interhemispheric temperature contrast on these seasonal timescales (panels b and c of what is now Figure 9). We have also added a new Figure 10 which shows the annual and seasonal mean positions of the ITCZ in G1 and piControl in each model. This led to the important additional conclusion that the G1 scenario damps the seasonal migration of the ITCZ by preferentially cooling the summer hemisphere and creating an anomalous Hadley circulation that transports energy to the summer hemisphere and moisture in the opposite direction. To our knowledge, this mechanism has not been discussed before or shown to exist the GeoMIP ensemble. It helps explain the finding of Tilmes et al. (2013) that summer monsoon precipitation is reduced in G1 in various regions, and presents an additional risk that needs to be considered related to implementation of solar geoengineering.

There are many comments in the attached annotated manuscript that need to be addressed.

- The typographical errors have been edited.
- One comment in the annotated manuscript asks, "Is it correct to categorize all precipitation processes this way? Is it atmospheric dynamics that changes precipitation microphysics or cloud thickness or lapse rate?" regarding our sentence: 'P-E changes not captured by this scaling are driven by non-thermodynamic mechanisms, including changes in relative humidity or atmospheric dynamics."

Decomposing the hydrological response to a climate forcing into thermodynamic and dynamic components is not the only possible way to understand the system of course, but it is a useful approach that has been fruitfully employed in other contexts (i.e., Seager et al. 2010; Wills et al. 2016; Li and Li 2014).

- Page 2, Line 29 of original manuscript: P-E over continents sets the total runoff, which includes the water flux that penetrates the surface. This has been clarified in the revised text. P-E is indeed a key factor in setting the salinity of the mixed layer and is not merely a coastal effect as you suggest, so we kept this part of the sentence intact. A citation to Byrne and O'Gorman (2015) was added here.
- Page 2, Line 30 of original manuscript: We provide the citation of the Held and Soden (2006) paper in which the P-E thermodynamic scaling is derived.
- Page 3, Line 26 of original manuscript: The comment is "Scaling is a statistical simplification. But what is physically going on? Scaling cannot predict anything. Why would you expect the physics of the situation to behave this way?"
  The P-E scaling is ultimately rooted in the Clausius-Clapeyron scaling of saturation vapor pressure with temperature. We discuss this in the beginning of Section 2.1.
- Page 3, line 28 comment: "Kravitz et al. (2013) already found this. And in the Tropics there is cooling. You need to reference previous work." We have added a citation here.
- Page 4 lines 1-2: We have added text to explain why thermodynamic scaling predicts an increase in P-E in G1-piControl. Thermodynamic scaling is based on the expectation that water vapor will increase in the atmosphere where there is warming (due to the Clausius-Clapeyron scaling of saturation vapor pressure and the assumption of constant RH), and thus that the P-E will increase in these regions. It is therefore not surprising that the thermodynamic scaling calculation results in P-E enhancement over regions with positive temperature anomalies.
- Page 4 line 8: We now define the ITCZ acronym in the Abstract.
- Page 4 line 11: The ECEARTH output files are faulty and log impossibly large precipitation values across most of the planet.
- Page 4 line 22: Edited to clarify.
- Page 7 line 5: "This is not a new finding. And why don't you show the seasonal cycle, which does not average out the interesting physics?" We now present the seasonal cycle of the Hadley circulation changes (Figs. 7, 8) as well as seasonal analysis on the ITCZ shifts (Figs. 9, 10). This paper is the first to present Hadley circulation changes in the G1 experiment.
- We have added a column with references for each model to Table 1.

In addition: I am confused. The text says there were 13 models and you excluded one, but do not say which model and why. Then Figs. 2 and 3 used 11 models, but excluded one. Again, what was the criterion for excluding the model? Table 1 only lists 12 models.

We did not have access to all of the data for CSIRO. In addition, the precipitation results for ECEARTH were not saved properly and could not be analyzed (δP values >>2 mm/day over most latitudes). We now include this information in the Introduction.

Fig. 1 is not a new result. It is the same as Fig. 2 (top right) of Kravitz et al. (2013a), and this needs to be acknowledged. Figs. 2 and 3 are not new. They are the same as Fig. 5 of Kravitz et al. (2013a), and this needs to be acknowledged.

These provide background for the novel work which comprises the vast majority of the paper, including figures and discussion, as addressed above.

I don't understand which results are plotted in Fig. 4A. Is it G1? piControl? The difference? The caption just says "as simulated in the models." If it is the difference, why does it differ from the results shown in Fig. 1 of Kravitz et al. (2103a), and again not acknowledged?

Fig. 4A is a new result, and is different from Fig. 1 of Kravitz et al. (2013a) because they plot the P-E anomaly over land only (see their caption). All four panels of Figure 4 are P-E anomalies (G1-Preindustrial). The caption has been edited to clarify this.

Graphics are poor quality. For Figs. 1-3, 5: - The color shading has way too many shades, so it is impossible to determine the value by looking at a color on the map. Use fewer values and include labeled contour lines.

We have reduced the number of colors on the color bars in Figs. 1-3, 5 to make the results more apparent without visual strain.

- The stippling is much too dense. It is impossible to see the shading underneath it.

The stippling denotes areas where fewer than ~64% of models agree on the sign of the change, so it is not important to see the shading underneath it. The regions with higher model agreement are intentionally emphasized.

- The x-axis label is wrong. The scaling is wrong and the longitude labels are in the wrong place. The right end should be 0∘. - The entire figure is blurry and too low resolution.

Thank you for pointing out that some of the longitude labels were misplaced. This has been corrected. With the changes to the color bar noted above, the figures are clear and easily readable.

- The criterion for shading varies from 62.5% to 64% to 66% agreement. Why? Why not use the 75% criterion of Kravitz et al. (2013a), which covers less of the data? - Try using GrADS. It makes beautiful maps, and automatically gives you labeling, contours, and shading.

The criterion for shading varies from 62.5% to 64% to 66% because the number of ensemble members among the figures varies based on data availability. All necessary exclusions were noted in figure captions. The temperature ensemble mean includes 12 models, while the rest include 11 models due to the exclusion of EC-EARTH. The relative humidity ensemble mean includes eight models. We reached out to scientists from all the modeling groups whose data

was not available on public servers, but not everyone was able to provide the surface relative humidity.

The 75% criterion would actually cover more of the data, because it would stipple all regions for which fewer than 75% of models agree on the sign of the change, rather than the regions where fewer than ~64% of the models agree. For the purpose of conveying the scientific content, a higher resolution image will not make a worthwhile difference, as the figures are already highly legible. I will try to use GrADS for future work.

For Fig. 6, the color shading has way too many shades, so it is impossible to determine the value by looking at a color on the map. Use fewer values and include labeled contour lines. Use "piControl" rather than "Preindustrial," as it is the standard CMIP5 terminology.

We have reduced the number of colors in this figure and in the new JAS and JFM streamfunction figures in order to facilitate understanding. We now use the shorthand "piControl" in much of the paper.

References not already included in paper

Li, L. & Li, W. *Clim Dyn* (2015) 45: 67. doi:10.1007/s00382-014-2216-3

Seager, R., N. Naik, and G. Vecchi, 2010: Thermodynamic and Dynamic Mechanisms for Large-Scale Changes in the Hydrological Cycle in Response to Global Warming. *J. Climate,* **23**, 4651–4668, doi: 10.1175/2010JCLI3655.1.

Wills, R. C., M. P. Byrne, and T. Schneider (2016), Thermodynamic and dynamic controls on changes in the zonally anomalous hydrological cycle, *Geophys. Res. Lett*., 4640–4649, doi: 10.1002/2016GL068418.

Thermodynamic and dynamic responses of the hydrological cycle to solar dimming

Jane E. Smyth[1], Rick D. Russotto[2], and Trude Storelvmo[1]

[1]Department of Geology & Geophysics, Yale University, New Haven, Connecticut, USA
[2]Department of Atmospheric Sciences, University of Washington, Seattle, Washington, USA

Correspondence to: Jane E. Smyth (jsmyth@princeton.edu)

Abstract. The fundamental role of the hydrological cycle in the global climate system motivates thorough evaluation of its responses to climate change and mitigation. The Geoengineering Model Intercomparison Project (GeoMIP) is a global collaboration that aims to assess the climate impacts of solar geoengineering, a proposal to counteract global warming with a reduction of incoming solar radiation. We assess the mechanisms underlying the rainfall response to a simplified simulation of solar dimming (G1) in the suite of GeoMIP models and identify robust features. While solar geoengineering nearly restores preindustrial temperatures, the global hydrology is altered. Tropical precipitation changes dominate the response across the model suite, and these are driven primarily by shifts of the Hadley circulation cells. We report a damping of the seasonal migration of the intertropical convergence zone (ITCZ) in G1, associated with preferential cooling of the summer hemisphere, and annual mean ITCZ shifts in some models that are correlated with warming of one hemisphere relative to the other. These dynamical changes cause greater rainfall anomalies than local changes in relative humidity or the Clausius-Clapeyron scaling of precipitation minus evaporation. The role of relative humidity, though small in the zonal mean, could be locally important over land, and is likely related to the CO_2 physiological response in plants. The variations among models in the movement of the intertropical convergence zone highlights the need for cautious consideration and continued study before any implementation of solar geoengineering.

1 Introduction

Solar geoengineering has been suggested as a way to counter the effects of global warming induced by anthropogenic greenhouse gas emissions (e.g., Crutzen, 2006; Robock et al., 2009). By reducing incoming solar radiation, solar geoengineering would bring the climate with elevated concentrations of CO_2 into radiative balance. It compensates for a change in surface temperature from increased CO_2 trapping of outgoing longwave radiation with a reduction of incoming shortwave radiation. Solar geoengineering is a controversial proposal, but should it come into favor due to continued greenhouse gas emissions, it is critical that the climate effects be understood before deployment (NRC, 2015).

The Geoengineering Model Intercomparison Project (GeoMIP) is intended to determine robust responses of the climate to various simulations of solar geoengineering, in experiments that range from simple representations of the solar dimming, to realistic representations of stratospheric aerosol emissions or marine cloud brightening (Kravitz et al., 2010). The GeoMIP

experiments are based on the Coupled Model Intercomparison Project Phase Five (CMIP5), which is a protocol for experiments using coupled atmosphere-ocean climate models (Table 1). The GeoMIP G1 experiment counteracts the forcing from quadrupled atmospheric CO_2 levels with a simple reduction of the solar constant across all wavelengths. The G1 experiment was run from the steady state preindustrial control (piControl) run, followed by an abrupt quadrupling of CO_2, and a simultaneous solar constant reduction for 50 years. The idealized nature of this simulation is conducive to multimodel comparison. It superimposes two large and opposite climate forcings, which offset one another nearly completely in terms of global mean net radiation balance at the top of the atmosphere and near-surface atmospheric temperature, but do not cancel in their hydrological effects, especially on local scales (Kravitz et al., 2013c).

Thirteen fully coupled models participated in the G1 experiment, though we did not have access to the data from the CSIRO model and it is not included in the present study. There are serious errors in the precipitation output files from the EC-EARTH model and it is thus excluded from any analysis involving the precipitation field. The models differ in their ocean, ice sheet, land surface and atmospheric components. The latter two components are particularly relevant for this study. Some, but not all models, feature dynamic vegetation distributions. The 11 models include a wide range of parametrizations and configurations, allowing for strong conclusions about robust climate responses that appear across models (Kravitz et al., 2013a).

The water cycle impacts agriculture, economies, as well as the welfare of ecosystems and human civilizations (IPCC, 2014). It is imperative to understand the effects of solar geoengineering on global hydrology, to evaluate whether the risks or unintended consequences of such an approach to climate change mitigation are likely to outweigh the benefits. To help improve our understanding of this issue, we analyze the contributions of several different effects to changes in precipitation minus evaporation ($P - E$) in the GeoMIP G1 experiment, as follows.

1. In Section 2.1, we analyze the thermodynamic response of $P - E$ to geoengineering.

2. In Section 2.2, we assess the role of changes in relative humidity on $P - E$.

3. In Section 2.3, we investigate the extent to which atmospheric circulation patterns, namely changes in the Hadley cell strength and position, drive $P - E$ changes in the models on both annual and seasonal timescales.

2 Analysis & Results

2.1 Thermodynamic Scaling of $P - E$

Precipitation minus evaporation determines the amount of subsurface and surface runoff on land, and is crucial in setting the salinity of the mixed layer over ocean (Byrne and O'Gorman 2015). We here discuss the component of $P - E$ changes driven by residual surface temperature changes (G1- piControl). Surface heating increases the temperature and the evaporation rate, which increases the atmospheric moisture content, or specific humidity q (Trenberth, 1999). We have confidence about certain aspects of the hydrological cycle's response to greenhouse gas warming, particularly those tightly coupled to the increase in saturation vapor pressure with warming (Held and Soden, 2006). The Clausius-Clapeyron expression (Eq. (1)), where R is

the gas constant, L the latent heat of vaporization, and α is the Clausius-Clapeyron scaling factor, relates the derivative of the natural log of saturation vapor pressure e_s with respect to temperature (T) to temperature itself.

$$\frac{d\ln e_s}{dT} = \frac{L}{RT^2} \equiv \alpha(T) \tag{1}$$

At typical near-surface temperatures, saturation vapor pressure increases at $7\ \%\text{K}^{-1}$.

5   Precipitation minus evaporation follows Clausius-Clapeyron scaling, as in Eq. (2), given three important assumptions (Held and Soden, 2006).

$$\delta(P - E) = \alpha\,\delta T\,(P - E) \tag{2}$$

First, it assumes small meridional gradients of temperature relative to $P - E$. Second, the relationship assumes no change in near-surface relative humidity between climate states. Third, it assumes that there is no change in the atmospheric flow. Though it is known that relative humidity and atmospheric circulation are not constant in a changing climate, the thermodynamic scaling is a useful way to represent the role of a simple physical mechanism (i.e. the Clausius-Clapeyron scaling of saturation vapor pressure with temperature) on global $P - E$ anomalies (Byrne and O'Gorman, 2015). This thermodynamic scaling equation represents the component of $P - E$ change driven directly by surface temperature perturbations. $P - E$ changes not captured by this scaling are driven by non-thermodynamic mechanisms, including changes in relative humidity or atmospheric dynamics.

15   This study evaluates the extent to which the basic physical relation between saturation vapor pressure and temperature accounts for the hydrological response to a combination of large-magnitude forcings: greenhouse gas warming and solar dimming.

We investigate how well thermodynamic scaling predicts hydrologic changes in a geoengineered climate for each model by comparing the prediction using Eq. (2) to the annual and zonal mean $P - E$ anomaly between G1 (years 11-50) and piControl (all years) in the model simulations. We also consider the annual-mean global distribution of precipitation minus evaporation anomalies. To better understand the contribution of relative humidity changes to the $P - E$ response, we also calculated an "extended scaling" adapted from Byrne and O'Gorman (2015). Our extended scaling includes the first two terms from Byrne and O'Gorman's equation,

$$\delta(P - E) = \alpha\,\delta T\,(P - E) + \frac{\delta H_s}{H_s}(P - E) \tag{3}$$

25   where H_s is the relative humidity at the surface. The calculation takes local changes in H_s into account, but for the sake of simplicity it excludes changes in the horizontal gradients of H_s. We calculated the difference between the zonal mean $P - E$ anomalies in the extended and simple scalings to quantify the influence of changes in H_s. We also calculated the difference between simulated $P - E$ anomalies and the extended thermodynamic scaling, to isolate the role of dynamics in the simulated hydrological response. Data for this analysis and the relative humidity analysis in Section 2.2 were unavailable for CESM, HadC, and MPI due to limited functionality of the central GeoMIP model data server, the Earth System Grid Federation (ESGF).

To provide reference points for our analysis, we have re-plotted some thermodynamic variables in Figures 1-3 that originally appeared in the G1 overview paper by Kravitz et al. (2013a). The experimental design results in minimal temperature anomalies between G1 (years 11-50) and piControl(all years) (Fig. 1), but does not eliminate hydrological effects (Fig. 2). The ensemble mean change in $P - E$ shows greater hydrological changes (up to 1 mm/day) in the tropics than at higher latitudes (Fig. 2). Figure 3, which separates the precipitation and evaporation changes from solar dimming, reveals that most of the spatial structure in the $P - E$ anomaly comes from the precipitation change.

The thermodynamic scaling captures virtually no change in global $P - E$ patterns, since by experimental design the temperature anomaly is minimal between the G1 and piControl scenarios (Fig. 4B). Temperature anomalies between G1 and the piControl show variations within 1 K, with some residual warming at high latitudes and cooling at low latitudes as a robust feature across the suite (Fig. 1) (Kravitz et al. 2013a). Such temperature anomalies are generally not sufficient to generate appreciable thermodynamic changes in P-E. The ensemble mean simulated precipitation minus evaporation anomaly deviates from the thermodynamic scaling by up to 1.0 mm/day and is highest in the tropics (Fig. 2). In the tropics,temperature anomalies are minimal compared to those at high northern latitudes and thus thermodynamic scaling does not account for the hydrological change. In BNU-ESM, thermodynamic scaling predicts a $P - E$ enhancement over the anomalously warm high latitudes, where the temperature response to quadrupled CO_2 levels is poorly compensated by solar dimming (annual mean G1-piControl anomalies >2K at polar latitudes, results not shown here).

The ensemble mean reflects strong reductions in precipitation in the subtropics (Fig. 3). Previous research has suggested that this is a result of the nature of the G1 experiment forcing. Solar geoengineering might suppress tropical precipitation since the reduction in shortwave radiation cools the surface more than the mid-troposphere, increasing atmospheric stability and reducing convection (Bala et al., 2008). However, looking at the zonal patterns for individual models, there are stronger hydrological effects that cancel out in the ensemble mean (Fig. 4A). The HadCM3, HadGEM2-ES, and CESM-Cam5.1-FV models show P-E anomalies indicating a northward shift in the Intertropical Convergence Zone (ITCZ), while those of GISS-E2-R, Can-ESM2, and MIROC-ESM demonstrate a southward shift. Annual mean anomalies in the zonal mean $P - E$ exceed 0.6 mm/day in the GISS-E2-R and HadGEM2-ES simulations. In CCSM4, IPSL-CM5A-LR, and NorESM1-M models, the ITCZ appears to narrow, with precipitation increasing at the equator and decreasing within 10°N and 10°S.

The deviations of the extended scaling from the simple scaling are less than 0.1 mm/day in all models (Fig. 4C). This demonstrates that local changes in relative humidity under solar dimming play a modest role in the zonal mean $P - E$ response. Figure 4D indicates that most of the zonal mean $P - E$ anomalies are not captured by the Clausius-Clapeyron scaling or by local relative humidity changes. We interpret this component of the hydrological response to be driven by atmospheric circulation changes. To better understand the influence of relative humidity changes on smaller spatial scales, we investigate the global distribution of H_s changes in the following section. We will then investigate the dynamical changes in the tropics in Section 2.3.

2.2 Relative Humidity

The thermodynamic scaling described above assumes no changes in relative humidity between climate states. In this section, we assess the role that relative humidity changes play in the $P-E$ response to uniform solar dimming. Relative humidity is the ratio of actual vapor pressure to saturation vapor pressure ($\frac{e}{e_s}$), or almost equivalently, specific humidity to saturation specific humidity ($\frac{q}{q_s}$). It can change with the water availability or temperature, with the latter affecting the saturation vapor pressure as in Eq. (1). The near-surface atmosphere provides moisture to the free troposphere, where water vapor plays an important role in radiative transfer, the hydrological cycle, and climate sensitivity (Willett et al., 2010). The near-surface relative humidity parameter is also of interest in climate change studies for evaluating the risk of human heat stress, under both high and low H_s extremes (Sherwood et al., 2010; Souch and Grimmond, 2004).

The assumption of constant relative humidity in the simple thermodynamic scaling of $P-E$ (Eq. (2)) relies on the availability of moisture. In a moisture-limited regime (i.e., over land) q may not increase proportionally with temperature, breaking the assumption of constant relative humidity. Under this circumstance, relative humidity adjustments would contribute to non-thermodynamic changes in the $P-E$ between climate states. An observational study found decreasing surface relative humidity from 1998-2008 over low and midlatitude land areas due to inhomogeneities in surface heating and moisture availability (Simmons et al., 2010). While relative humidity has been found to be nearly constant in global warming simulations with high vertical resolution (Allen and Ingram, 2002), the assumption of constant H_s may not be sound when insolation rather than temperature is perturbed, as in the G1 experiment.

We consider the absolute changes in the relative humidity distribution to explain precipitation anomalies between G1 (years 11-50) and piControl (all years) simulations unaccounted for by thermodynamic or dynamic mechanisms. As noted in Section 2.1, the relative humidity data were unavailable for the CESM, HadC, and MPI models due to limited functionality of the ESGF data server. In six of the eight models presented here, relative humidity is reduced over land and conserved over ocean (Fig. 5). The relative humidity reductions are largest over tropical South America and sub-Saharan Africa. The reductions are up to 15% (0.15) in GISS-E2-R and HadGEM2-ES (calculated as the G1 relative humidity (%) minus the piControl relative humidity (%)). The CO_2 physiological effect is included in the land models of 11 GeoMIP simulations, all but EC-Earth (Table 1). In response to elevated ambient CO_2 concentrations, plants constrict their stomata, which reduces evapotranspiration in the high CO_2 simulations, including the G1 simulations (Kravitz et al., 2013c; Cao et al., 2010). In the global warming (abrupt4xCO2) GeoMIP simulations, this effect is partially offset by the increased net primary productivity in a warmer world. However, in G1, this net primary productivity effect is muted by the reduction in insolation. Tilmes et al. (2013) found that the physiological response to G1 is qualitatively the same as for abrupt4xCO2. Biogeochemical cycling has been found to influence global precipitation as much as the radiative reduction itself (Fyfe et al., 2013).

Bala et al. (2008) investigated changes in global mean precipitation in a single climate model. They noted a greater hydrological sensitivity to solar versus greenhouse forcing and attributed it to global energy budget constraints. Solar forcing heats the surface directly, while greenhouse forcing heats the troposphere. Changes in the insolation therefore have a greater effect on surface net radiation fluxes (i.e., latent and sensible heat fluxes change more than in the CO_2 case). When the downward

shortwave flux decreases, the surface fluxes must respond, and in this case the latent heat flux dominates the response. Evaporation decreases, and precipitation follows. Bala et al. do not address how this global mean equilibrium constraint will manifest regionally, but our analysis (e.g. Fig 3) is consistent with this reasoning.

In the National Center for Atmospheric Research (NCAR) Community Land and Community Atmosphere Model, Cao et al.
(2010) isolated the CO_2 physiological effect from a doubling of atmospheric CO_2. They reported patterns of reduced latent heat flux and relative humidity from this vegetative forcing that closely resemble those we observe in the GeoMIP suite, in Fig. 3 and Fig. 5. In the present study, since strong and significant reductions in relative humidity over land are largely constrained to regions with extensive vegetation in the form of boreal, temperate or tropical forests, we consider the biogeochemical effect of CO_2 to be the dominant cause of the relative humidity change. The role of these biogeochemical H_s changes is minimal in
zonal mean climate (Fig. 4C) but could have significant influence at smaller spatial and temporal scales.

2.3 Dynamically Driven Precipitation

The third factor we consider in decomposing the $P - E$ response to geoengineering is the atmospheric circulation. Large-scale meridional circulations are driven by energy gradients imposed by the uneven distribution of sunlight on Earth. The Hadley circulation cells are responsible for most of the poleward heat transport in the tropics, where the annual solar input is highest
(Hill et al., 2015). The net energy flux of the Hadley circulation is in the flow direction of its upper branch (Held, 2001). The ascending motion of the Hadley cell drives the seasonally-migrating tropical rainfall known as the ITCZ, and there is evidence that its position is determined by meridional gradients in the vertically-integrated atmospheric energy budget (Shekar and Boos, 2016). The Hadley circulation is crucial for balancing global energy, so high-latitude temperature anomalies can drive shifts of the ITCZ (Yoshimori and Broccoli, 2008). The ITCZ is sensitive to interhemispheric energy contrasts set up by
aerosols, clouds, or antisymmetric heating (Seo et al., 2014). A thorough analysis of Hadley circulation changes is a crucial outstanding task for understanding the hydrological response to solar geoengineering (Kravitz et al., 2013c). We will quantify changes to the Hadley circulation with the meridional streamfunction. The meridional streamfunction is derived from the continuity equation, and either $\bar{v}$, the meridional wind vector, or $\bar{w}$, the vertical wind vector, can be used to fully define the two-dimensional, overturning flow (Eq. (4)):

$$\Psi(\phi, p) = 2\pi a \cos\phi \int_0^p \bar{v} \, dp/g. \tag{4}$$

where ϕ is the latitude, p is pressure, a is the Earth's radius, $\bar{v}$ is the meridional velocity, and g is gravity.

Changes in TOA energy fluxes influence the direction and strength of ITCZ shifts (Kang et al., 2008). Numerous studies have noted the strong relationship between ITCZ position and the hemispheric temperature contrast as well. The correlation between interhemispheric temperature contrasts and annual mean ITCZ position is a robust result and is related to extratropical
energy transport (e.g., Broccoli et al., 2006; Toggweiler and Lea, 2010). Schneider et al. (2014) explain how this is consistent with an energetic framework: the hemisphere with the higher average temperature typically has a smaller meridional temper-

6

ature gradient due to the near symmetry of tropical temperatures about the equator. This corresponds to reduced poleward extratropical eddy transport in that hemisphere, and increased energy flux by the atmosphere across the equator and out of the hemisphere by the upper branch of the Hadley cell. The ITCZ is drawn towards the warmed hemisphere because moisture is transported in the opposite direction as energy by the Hadley cell. Therefore, we investigate the possibility that differing

5   dynamical responses to solar dimming among the models are due to differences in the temperature restoration of the Northern and Southern Hemispheres.

To discern the component of the precipitation change caused by changes in large scale atmospheric dynamics, we calculated the change in the Hadley circulation between the G1 (years 11-50) and piControl (final 40 years) simulations. For each model, we computed the meridional streamfunction over this 40 year averaging period based on the modeled meridional wind vector,

10   as in Eq. (4). Data were unavailable for the CESM and HadC models. We examined annual and seasonal mean dynamical changes to analyze the changes in the zonal mean hydrological cycle, including the periods July-August-September (JAS) and January-February-March (JFM). To better interpret the dynamical changes, we assessed the annual mean and seasonal changes in the interhemispheric temperature contrast between G1 and piControl for each model by calculating area-weighted hemispheric averages of the surface temperature, averaged over a 40 year period (years 11-50 of G1 and 1-40 of piControl).

15   The ITCZ shift between G1 and piControl is defined as the shift of the precipitation centroid. This is the latitude between $15°N$ and $15°S$ at which half the precipitation is to the north and half is to the south.

The annual mean Hadley circulation changes vary in magnitude and direction amongst the GeoMIP ensemble members and contribute to dynamic moistening and drying. The meridional streamfunction plots suggest that the northward (HadGEM2-ES) and southward (GISS-E2-R, MIROC-ESM) ITCZ shifts, characterized by counterclockwise or clockwise tropical anomalies

20   respectively, are dynamically driven (Fig. 6). The anomalous ascent at the equator in CCSM4 and NorESM1-M accounts for the narrowing of the ITCZ noted in the zonal mean $P - E$ figure. The mean circulation does not seem to provide a dynamical basis for the annual mean constriction of the ITCZ in the MPI-ESM-LR and IPSL-CM5A-LR models, in which anomalies are less than 10^{10} kg s^{-1}. Small changes in the latitudinal range and strength of the Hadley circulation and associated precipitation have large local implications, especially on subannual scales (Kang et al., 2009). We find that summer (July-August-September, or

25   JAS) and winter (January-February-March, or JFM) meridional streamfunction anomalies are in every model stronger than the annual mean (Figs. 7, 8). In HadGEM2-ES, for example, the JAS meridional mass flux anomaly exceeds 4×10^{10} kg s^{-1}. On the opposite extreme, the IPSL-CM5A-LR model JAS and JFM mass flux anomalies are below 1.5×10^{10} kg s^{-1}. In general, the JAS streamfunction changes rather than the JFM anomalies set the pattern for the annual mean circulation change (Figs. 6-8). In the JAS average, there is anomalous energy transport toward the summer hemisphere (NH) in eight of nine models (all

30   but HadGEM) (Fig. 7). In the JFM average, there is again anomalous energy transport toward the summer hemisphere (SH), though the result is less consistent across the suite (seven of nine models) (Fig. 8). These changes in the Hadley cell mass flux are consistent with the relative cooling of the summer hemisphere throughout the year (Fig. 9b,c).

We find that the shifts of annual mean tropical rainfall in the models are correlated with the interhemispheric surface temperature contrasts (Correlation coefficient $(r) = 0.64$, Fig. 9a). Models with higher annual mean surface temperatures in the

35   Northern Hemisphere under geoengineering tend to display northward shifts of the ITCZ. This is consistent with previous

research that shows a strong relationship between the ITCZ position and the hemispheric temperature contrast (e.g., Kang et al., 2008; Frierson and Hwang, 2012). Modeling studies by Haywood et al. (2013, 2016) have shown that increasing the albedo by injecting stratospheric aerosols into only one hemisphere could cause substantial shifts in the ITCZ toward the other hemisphere. Our analysis of the G1 experiment suggests that similar effects could occur, albeit on a smaller scale, even with a

5   hemispherically symmetric injection strategy, which is approximated by reducing the solar constant. Despite the hemispherically symmetric forcing induced by solar dimming, the ensemble mean residual high-latitude warming is larger in the Arctic than in the Antarctic (Fig. 1), and in 9 out of 11 models the Northern Hemisphere is warmed relative to the Southern Hemisphere after geoengineering (Fig. 7a). This suggests that there could be an intriguingly close relationship between the degree of Arctic warming amplification and the tropical hydrological response to geoengineering in models. The relationship between

10   ITCZ shifts and energy transport in G1 will be further explored in a future study.

One response of the ITCZ to the G1 experiment that is consistent across all 11 models is that the seasonal migration of the ITCZ is dampened. Figure 10 shows the annual, boreal winter (JFM), and boreal summer (JAS) mean position of the ITCZ in each model in piControl (years 1-40) and G1 (years 11-50). In each model, the distance between the seasonal mean positions of the ITCZ is reduced. In some models there is a poleward shift in the ITCZ in one of the seasons, but in each of these cases

15   there is a greater equatorward shift in the opposite season, with an annual mean ITCZ shift and a reduction in the seasonal migration occurring simultaneously.

The reduction in the seasonal ITCZ migration is consistent with the physical mechanism relating sulfate aerosols and ITCZ shifts during 1971-1990 described by Hwang et al. (2013; see their Figure 4). There is more available sunlight in the summer hemisphere, which results in a greater cooling there when the solar constant is reduced. To compensate for the loss of energy

20   in the summer hemisphere, the climatological energy flux out of the summer hemisphere and towards the winter hemisphere is reduced. Indeed, in G1, most models show an anomalous Hadley circulation in which winds aloft, and therefore energy, move towards the summer hemisphere (Figs. 7,8). This is accompanied by anomalous flow towards the winter hemisphere in the lower branch of the Hadley cell, which weakens moisture transport towards the summer hemisphere and moves the summer ITCZ position away from the summer pole. The warming of the winter relative to the summer hemisphere and the ITCZ shift

25   toward the winter hemisphere are correlated between the different models (Fig. 9b,c), and are consistent with the proposed physical mechanism.

Damped seasonal ITCZ migration caused by cooling of the summer hemisphere presents a physical mechanism for the reduction in summer monsoon precipitation in the G1 experiment found by Tilmes et al. (2013), which they had attributed to a weakening of the hydrological cycle. It also provides an explanation for the narrowing of the annual mean ITCZ in the

30   IPSL-CM5A-LR and MPI-ESM-LR models that could not be accounted for by the annual mean dynamics. If this effect were to occur in the real world, it would likely mean a reduction in precipitation in areas that depend on the seasonal extremes of the ITCZ position for their rainfall, in both hemispheres. This is one more reason to be cautious about implementation of solar geoengineering. Future studies should look for this effect in model simulations that include actual aerosol injections, rather than reducing the solar constant, in order to learn more about this potential risk.

3   Conclusions

Hadley circulation changes are the most significant mechanism driving the $P - E$ changes in climate model simulations of uniform solar dimming. While thermodynamic scaling captures the general spatial structure of $P - E$ changes under global warming, it does not explain the large-scale rainfall changes in idealized simulations of solar geoengineering. The roles of thermodynamic scaling and relative humidity changes may be important on studies of smaller scale responses to geoengineering, such as over rainforests or at high latitudes where the CO_2 physiological response and residual temperature anomalies are more important, respectively.

The models can be divided into three groups characterized by different precipitation responses to geoengineering: either a southward shift, northward shift, or narrowing of the ITCZ. Our results support that changes in tropical dynamics, namely shifts of the Hadley circulation, are largely responsible for these alterations to the $P - E$ distribution. In a previous study, convection scheme parameters were determinative of the tropical precipitation response to extratropical forcings (Kang et al., 2009). The partitioning of cross-equatorial fluxes between atmospheric and oceanic components is also important for the resulting ITCZ shift, so differences in the oceanic component of the models could emerge as significant (Kang et al., 2008).

We also present evidence that land-sea contrasts in evaporation rates, resulting in land-sea contrasts in relative humidity anomalies, contribute to small changes in $P - E$ with solar dimming. We propose that these relative humidity changes are related to the effect of CO_2 on the stomatal conductance in plants.

This study demonstrates that tropical precipitation is sensitive to solar perturbations and would be altered by an implementation of solar geoengineering. The basis of this alteration is primarily dynamical. Based on our inter-model comparison, there is substantial uncertainty regarding the nature of the tropical precipitation response, in terms of the direction and strength of the ITCZ shift, as well as its variation on seasonal time scales. We present evidence that residual warming of one hemisphere relative to the other under geoengineering draws annual mean tropical rainfall into that hemisphere. On seasonal timescales, preferential cooling of the summer hemisphere results in a damping of the seasonal migration of the ITCZ, which explains the apparent narrowing of the tropical peak in annual mean precipitation and helps account for the reduction in summer monsoon precipitation found by Tilmes et al. (2013). Our results reinforce the finding that uniform solar dimming cannot restore preindustrial conditions in terms of $P - E$ patterns, a fundamental aspect of climate. An investigation of the ability of spatially targeted solar geoengineering to offset these $P - E$ changes would be a valuable future direction.

References

Allen, M. R. and Ingram, W. J.: Constraints on future changes in climate and the hydrologic cycle, Nature, 419, 224–232, 2002.

Arora, V. K., Scinocca, J. F., Boer, G. J., Christian, J. R., Denman, K. L., Flato, G. M., Kharin, V. V., Lee, W. G., and Merryfield, W. J.: Carbon emission limits required to satisfy future representative concentration pathways of greenhouse gases, Geophysical Research Letters, 38, L05805, doi:10.1029/2010GL046270, 2011.

5 Bala, G., Duffy, P., and Taylor, K.: Impact of geoengineering schemes on the global hydrological cycle, PNAS, 105, 7664–7669, 2008.

Bentsen, M., Bethke, I., Debernard, J. B., Iversen, T., Kirkevåg, A., Seland, Ø., Drange, H., Roelandt, C., Seierstad, I. A., Hoose, C., and Kristjánsson, J. E.: The Norwegian Earth System Model, NorESM1-M – Part 1: Description and basic evaluation of the physical climate, Geoscientific Model Development, 6, 687–720, doi:10.5194/gmd-6-687-2013, 2013.

10 Broccoli, A. J., Dahl, K. A., and Stouffer, R. J.: Response of the ITCZ to Northern Hemisphere cooling, Geophysical Research Letters, 33, doi:10.1029/2005GL024546, http://dx.doi.org/10.1029/2005GL024546, l01702, 2006.

Byrne, M. P. and O'Gorman, P. A.: The Response of Precipitation Minus Evapotranspiration to Climate Warming: Why the "Wet-Get-Wetter, Dry-Get-Drier" Scaling Does Not Hold over Land, Journal of Climate, 28, 8078–8092, doi:10.1175/JCLI-D-15-0369.1, 2015.

Cao, L., Bala, G., Caldeira, K., Nemani, R., and Ban-Weiss, G.: Importance of carbon dioxide physiological forcing to future climate change, 15 Proceedings of the National Academy of Sciences, 107, 9513–9518, doi:10.1073/pnas.0913000107, 2010.

Collins, W. J., Bellouin, N., Doutriaux-Boucher, M., Gedney, N., Halloran, P., Hinton, T., Hughes, J., Jones, C. D., Joshi, M., Liddicoat, S., Martin, G., O'Connor, F., Rae, J., Senior, C., Sitch, S., Totterdell, I., Wiltshire, A., and Woodward, S.: Development and evaluation of an Earth-System model – HadGEM2, Geoscientific Model Development, 4, 1051–1075, doi:10.5194/gmd-4-1051-2011, 2011.

Crutzen, P. J.: Albedo Enhancement by Stratospheric Sulfur Injections: A Contribution to Resolve a Policy Dilemma?, Climatic Change, 77, 20 211–220, doi:10.1007/s10584-006-9101-y, http://dx.doi.org/10.1007/s10584-006-9101-y, 2006.

Dufresne, J.-L., Foujols, M.-A., Denvil, S., Caubel, A., Marti, O., Aumont, O., Balkanski, Y., Bekki, S., Bellenger, H., Benshila, R., Bony, S., Bopp, L., Braconnot, P., Brockmann, P., Cadule, P., Cheruy, F., Codron, F., Cozic, A., Cugnet, D., de Noblet, N., Duvel, J.-P., Ethé, C., Fairhead, L., Fichefet, T., Flavoni, S., Friedlingstein, P., Grandpeix, J.-Y., Guez, L., Guilyardi, E., Hauglustaine, D., Hourdin, F., Idelkadi, A., Ghattas, J., Joussaume, S., Kageyama, M., Krinner, G., Labetoulle, S., Lahellec, A., Lefebvre, M.-P., Lefevre, F., Levy, C., Li, Z. X., 25 Lloyd, J., Lott, F., Madec, G., Mancip, M., Marchand, M., Masson, S., Meurdesoif, Y., Mignot, J., Musat, I., Parouty, S., Polcher, J., Rio, C., Schulz, M., Swingedouw, D., Szopa, S., Talandier, C., Terray, P., Viovy, N., and Vuichard, N.: Climate change projections using the IPSL-CM5 Earth System Model: from CMIP3 to CMIP5, Climate Dynamics, 40, 2123–2165, doi:10.1007/s00382-012-1636-1, 2013.

Frierson, D. and Hwang, Y.-T.: Extratropical Influence on ITCZ Shifts in Slab Ocean Simulations of Global Warming, Journal of Climate, 25, 720–733, doi:10.1175/JCLI-D-11-00116.1, 2012.

30 Fyfe, J., Cole, J., Arora, V., and Scinocca, J.: Biogeochemical carbon coupling influences global precipitation in geoengineering experiments, Geophys. Res. Letters, 40, 651–655, 2013.

Gent, P. R., Danabasoglu, G., Donner, L. J., Holland, M. M., Hunke, E. C., Jayne, S. R., Lawrence, D. M., Neale, R. B., Rasch, P. J., Vertenstein, M., Worley, P. H., Yang, Z.-L., and Zhang, M.: The Community Climate System Model Version 4, Journal of Climate, 24, 4973–4991, doi:10.1175/2011JCLI4083.1, 2011.

35 Giorgetta, M. A., Jungclaus, J., Reick, C. H., Legutke, S., Bader, J., Böttinger, M., Brovkin, V., Crueger, T., Esch, M., Fieg, K., Glushak, K., Gayler, V., Haak, H., Hollweg, H.-D., Ilyina, T., Kinne, S., Kornblueh, L., Matei, D., Mauritsen, T., Mikolajewicz, U., Mueller, W., Notz, D., Pithan, F., Raddatz, T., Rast, S., Redler, R., Roeckner, E., Schmidt, H., Schnur, R., Segschneider, J., Six, K. D., Stockhause, M.,

Timmreck, C., Wegner, J., Widmann, H., Wieners, K.-H., Claussen, M., Marotzke, J., and Stevens, B.: Climate and carbon cycle changes from 1850 to 2100 in MPI-ESM simulations for the Coupled Model Intercomparison Project phase 5, Journal of Advances in Modeling Earth Systems, 5, 572–597, doi:10.1002/jame.20038, 2013.

Gordon, C., Cooper, C., Senior, C. A., Banks, H., Gregory, J. M., Johns, T. C., Mitchell, J. F. B., and Wood, R. A.: The simulation of SST, sea ice extents and ocean heat transports in a version of the Hadley Centre coupled model without flux adjustments, Climate Dynamics, 16, 147–168, doi:10.1007/s003820050010, http://dx.doi.org/10.1007/s003820050010, 2000.

Haywood, J., Jones, A., Bellouin, N., and Stephenson, D.: Asymmetric forcing from stratospheric aerosols impacts Sahelian rainfall, Nature Climate Change, 1857, 1–6, 2013.

Haywood, J. M., Jones, A., Dunstone, N., Milton, S., Vellinga, M., Bodas-Salcedo, A., Hawcroft, M., Kravitz, B., Cole, J., Watanabe, S., and Stephens, G.: The impact of equilibrating hemispheric albedos on tropical performance in the HadGEM2-ES coupled climate model, Geophysical Research Letters, 43, 395–403, doi:10.1002/2015GL066903, http://dx.doi.org/10.1002/2015GL066903, 2015GL066903, 2016.

Hazeleger, W., Wang, X., Severijns, C., Ştefănescu, S., Bintanja, R., Sterl, A., Wyser, K., Semmler, T., Yang, S., van den Hurk, B., van Noije, T., van der Linden, E., and van der Wiel, K.: EC-Earth V2.2: description and validation of a new seamless earth system prediction model, Climate Dynamics, 39, 2611–2629, doi:10.1007/s00382-011-1228-5, 2012.

Held, I.: The Partitioning of the Poleward Energy Transport between the Tropical Ocean and Atmosphere, Journal of the Atmospheric Sciences, 58, 943–948, 2001.

Held, I. and Soden, B.: Robust responses of the hydrological cycle to global warming, Journal of Climate, 19, 5686–5699, 2006.

Hill, S., Ming, Y., and Held, I.: Mechanisms of Forced Tropical Meridional Energy Flux Change, Journal of Climate, 28, 1725–1742, 2015.

Hurrell, J. W., Holland, M. M., Gent, P. R., Ghan, S., Kay, J. E., Kushner, P. J., Lamarque, J.-F., Large, W. G., Lawrence, D., Lindsay, K., Lipscomb, W. H., Long, M. C., Mahowald, N., Marsh, D. R., Neale, R. B., Rasch, P., Vavrus, S., Vertenstein, M., Bader, D., Collins, W. D., Hack, J. J., Kiehl, J., and Marshall, S.: The Community Earth System Model: A Framework for Collaborative Research, Bulletin of the American Meteorological Society, 94, 1339–1360, doi:10.1175/BAMS-D-12-00121.1, 2013.

Hwang, Y.-T., Frierson, D. M. W., and Kang, S. M.: Anthropogenic sulfate aerosol and the southward shift of tropical precipitation in the late 20th century, Geophysical Research Letters, 40, 2845–2850, doi:10.1002/grl.50502, 2013.

IPCC: Climate Change 2014: Impacts, Adaptation, and Vulnerability. Part A: Global and Sectoral Aspects, p. 1132, Cambridge University Press, Cambridge, United Kingdom and New York, NY, USA, 2014.

Ji, D., Wang, L., Feng, J., Wu, Q., Cheng, H., Zhang, Q., Yang, J., Dong, W., Dai, Y., Gong, D., Zhang, R.-H., Wang, X., Liu, J., Moore, J. C., Chen, D., and Zhou, M.: Description and basic evaluation of Beijing Normal University Earth System Model (BNU-ESM) version 1, Geoscientific Model Development, 7, 2039–2064, doi:10.5194/gmd-7-2039-2014, http://www.geosci-model-dev.net/7/2039/2014/, 2014.

Kang, S., Held, I., Friersona, D., and Zhao, M.: The Response of the ITCZ to Extratropical Thermal Forcing: Idealized Slab-Ocean Experiments with a GCM, Journal of Climate, 21, 3521–3532, 2008.

Kang, S., Frierson, D., and Held, I.: The Tropical Response to Extratropical Thermal Forcing in an Idealized GCM: The Importance of Radiative Feedbacks and Convective Parameterization, Journal of the Atmospheric Sciences, 66, 2812–2827, 2009.

Kravitz, B., Robock, A., Boucher, O., Schmidt, H., and Taylor, K.: Specifications for GeoMIP experiments G1 through G4, Available online at http://climate.envsci.rutgers.edu/GeoMIP/docs/specificationsG1G4.pdf [accessed April 2016], 2010.

Kravitz, B., Caldeira, K., Boucher, O., Robock, A., Rasch, P. J., Alterskjær, K., Karam, D. B., Cole, J. N. S., Curry, C. L., Haywood, J. M., Irvine, P. J., Ji, D., Jones, A., Kristjánsson, J. E., Lunt, D. J., Moore, J. C., Niemeier, U., Schmidt, H., Schulz, M., Singh, B., Tilmes, S.,

Watanabe, S., Yang, S., and Yoon, J.-H.: Climate model response from the Geoengineering Model Intercomparison Project (GeoMIP), JGR: Atmospheres, 118, 8320–8332, 2013a.

Kravitz, B., Rasch, P. J., Forster, P. M., Andrews, T., Cole, J. N. S., Irvine, P. J., Ji, D., Kristjánsson, J. E., Moore, J. C., Muri, H., Niemeier, U., Robock, A., Singh, B., Tilmes, S., Watanabe, S., and Yoon, J.-H.: An energetic perspective on hydrological cycle changes in the Geoengineering Model Inter-Comparison Project, JGR: Atmospheres, 118, 13,087–13,102, 2013c.

NRC: Front Matter. Climate Intervention: Reflecting Sunlight to Cool Earth, Washington, DC: The National Academies Press, doi:10.17226/18988, 2015.

Robock, A., Marquardt, A., Kravitz, B., and Stenchikov, G.: Benefits, risks, and costs of solar geoengineering, Geophysical Research Letters, 36, 2009.

Schmidt, G. A., Kelley, M., Nazarenko, L., Ruedy, R., Russell, G. L., Aleinov, I., Bauer, M., Bauer, S. E., Bhat, M. K., Bleck, R., Canuto, V., Chen, Y.-H., Cheng, Y., Clune, T. L., Del Genio, A., de Fainchtein, R., Faluvegi, G., Hansen, J. E., Healy, R. J., Kiang, N. Y., Koch, D., Lacis, A. A., LeGrande, A. N., Lerner, J., Lo, K. K., Matthews, E. E., Menon, S., Miller, R. L., Oinas, V., Oloso, A. O., Perlwitz, J. P., Puma, M. J., Putman, W. M., Rind, D., Romanou, A., Sato, M., Shindell, D. T., Sun, S., Syed, R. A., Tausnev, N., Tsigaridis, K., Unger, N., Voulgarakis, A., Yao, M.-S., and Zhang, J.: Configuration and assessment of the GISS ModelE2 contributions to the CMIP5 archive, Journal of Advances in Modeling Earth Systems, 6, 141–184, doi:10.1002/2013MS000265, 2014.

Schneider, T., Bischoff, T., and Huag, G.: Migrations and dynamics of the intertropical convergence zone, Nature Review, 513, 45–53, 2014.

Seo, J., Kang, S., and Frierson, D.: Sensitivity of Intertropical Convergence Zone Movement to the Latitudinal Position of Thermal Forcing, Journal of Climate, 27, 3035–3042, 2014.

Shekar and Boos: Improving Energy-Based Estimates of Monsoon Location in the Presence of Proximal Deserts, Journal of Climate, 29, 2016.

Sherwood, S. C., Ingram, W., Tsushima, Y., Satoh, M., Roberts, M., Vidale, P. L., and O'Gorman, P. A.: Relative humidity changes in a warmer climate, Journal of Geophysical Research: Atmospheres, 115, doi:10.1029/2009JD012585, 2010.

Simmons, A. J., Willett, K. M., Jones, P. D., Thorne, P. W., and Dee, D. P.: Low-frequency variations in surface atmospheric humidity, temperature, and precipitation: Inferences from reanalyses and monthly gridded observational data sets, Journal of Geophysical Research: Atmospheres, 115, doi:10.1029/2009JD012442, 2010.

Souch, C. and Grimmond, C.: Applied climatology:heat waves', Progress in Physical Geography, 28, 599–606, 2004.

Tilmes, S., Fasullo, J., Lamarque, J.-F., Marsh, D. R., Mills, M., Alterskjær, K., Muri, H., Kristjánsson, J. E., Boucher, O., Schulz, M., et al.: The hydrological impact of geoengineering in the Geoengineering Model Intercomparison Project (GeoMIP), Journal of Geophysical Research: Atmospheres, 118, 2013.

Toggweiler, J. R. and Lea, D. W.: Temperature differences between the hemispheres and ice age climate variability, Paleoceanography, 25, doi:10.1029/2009PA001758, http://dx.doi.org/10.1029/2009PA001758, pA2212, 2010.

Trenberth, K.: Atmospheric Moisture Recycling: Role of Advection and Local Evaporation, Journal of Climate, 12, 1368–1381, 1999.

Watanabe, S., Hajima, T., Sudo, K., Nagashima, T., Takemura, T., Okajima, H., Nozawa, T., Kawase, H., Abe, M., Yokohata, T., Ise, T., Sato, H., Kato, E., Takata, K., Emori, S., and Kawamiya, M.: MIROC-ESM 2010: model description and basic results of CMIP5-20c3m experiments, Geoscientific Model Development, 4, 845–872, doi:10.5194/gmd-4-845-2011, 2011.

Willett, K., Jones, P., Thorne, P., and Gillett, N.: A comparison of large scale changes in surface humidity over land in observations and CMIP3 general circulation models, Environmental Research Letters, 5, 025 210, 2010.

FIGURES
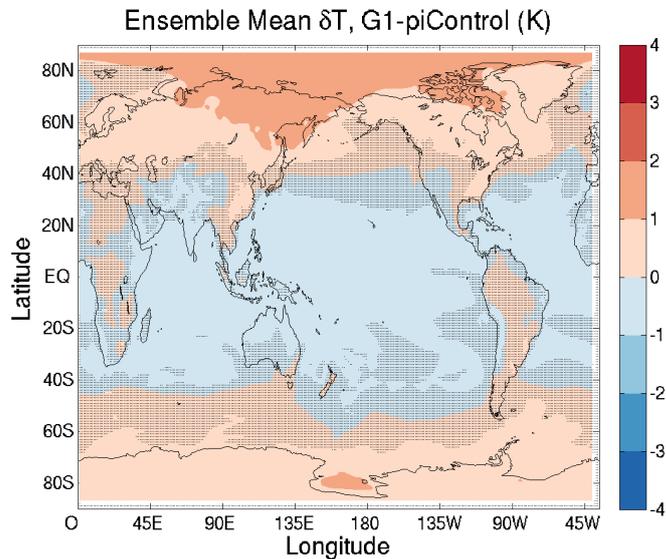
Figure 1. The annual mean distribution of near-surface atmospheric temperature anomalies (K) between G1 (years 11-50) and piControl (all years). Stippling denotes regions where fewer than 66% of the 12 ensemble members agree on the sign of the change. These results appear in Kravitz et al. 2013a.
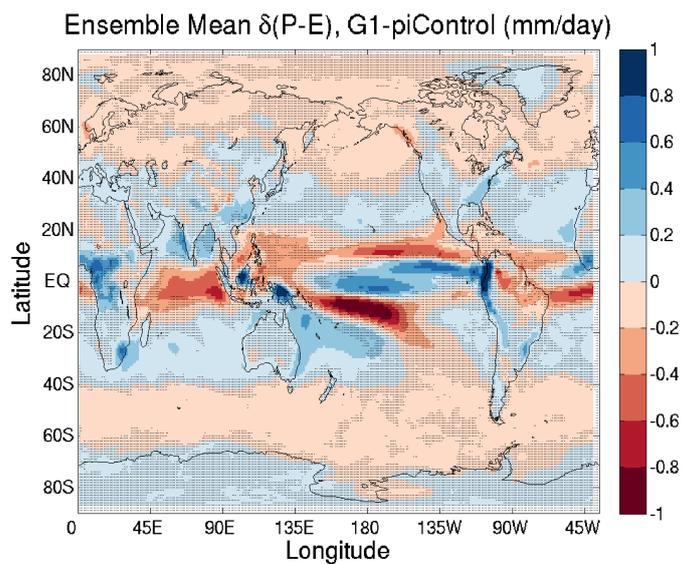
Figure 2. The annual mean distribution of precipitation minus evaporation rate anomalies (mm/year) between G1 (years 11-50) and piControl (all years), averaged among 11 models (EC-Earth excluded due to unphysical result). Stippling indicates where fewer than 64% of models agree on the sign of the change. These results appear in Kravitz et al. 2013a.
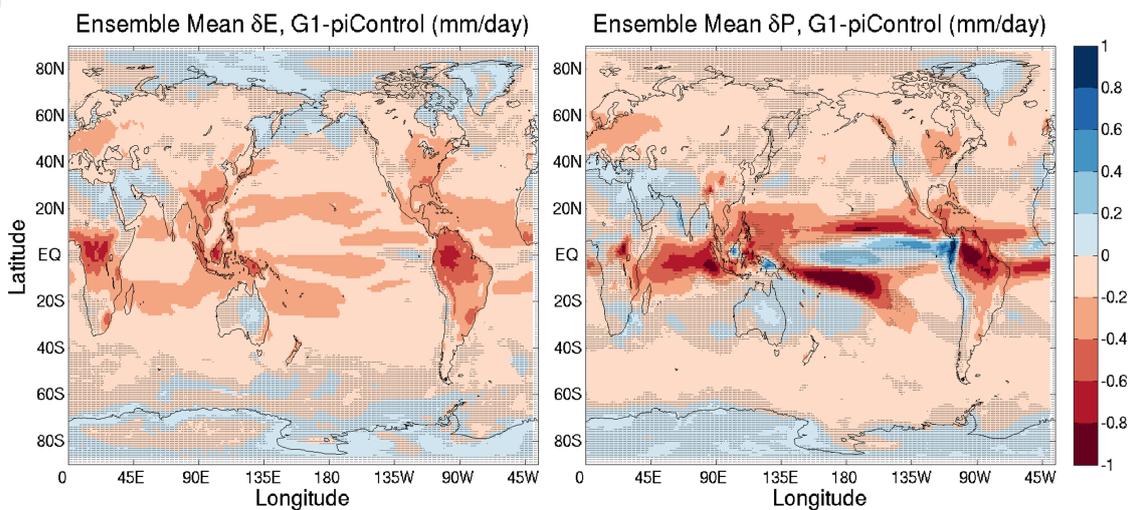

Figure 3. The annual mean distribution of evaporation (left panel) and precipitation (right panel) rate anomalies (mm/year) between G1 (years 11-50) and piControl (all years), averaged among 11 models (EC-Earth excluded due to unphysical result). Stippling indicates where fewer than 64% of models agree on the sign of the change. These results appear in Kravitz et al. 2013a.

15
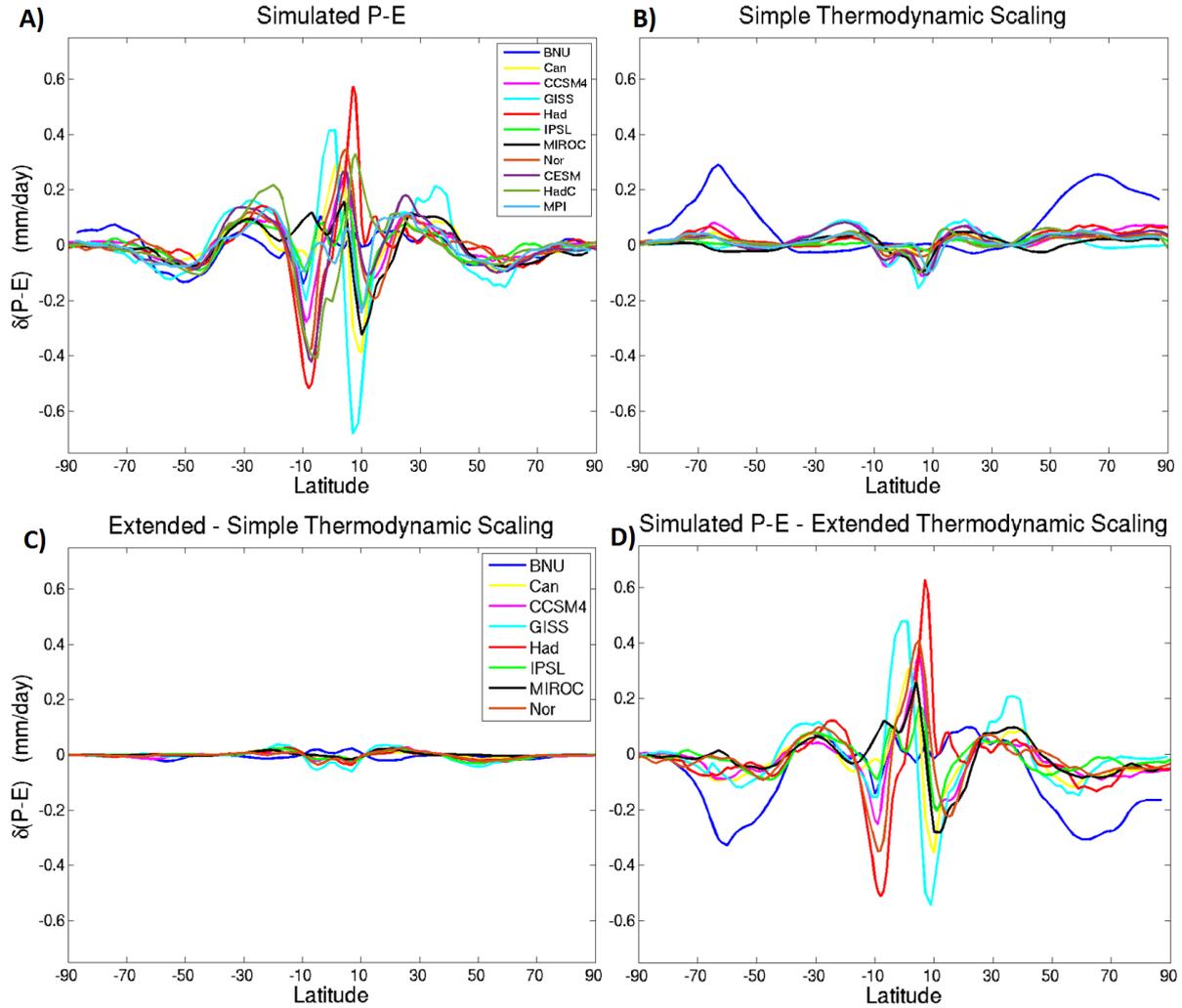
Figure 4. A) shows the zonal mean $P - E$ anomaly G1-piControl simulated in 11 climate models, and B) is the $P - E$ anomaly predicted by the simple thermodynamic scaling in Eq. (2). C) shows the $\delta P - E$ difference between the extended (Eq. (3)) and simple (Eq. (2)) scalings. This isolates the contribution of local relative humidity changes to the $P - E$ anomalies. D) is the difference between the simulated $\delta P - E$ and the extended scaling, and represents the changes in dynamically driven rainfall. (EC-Earth excluded due to unphysical result).
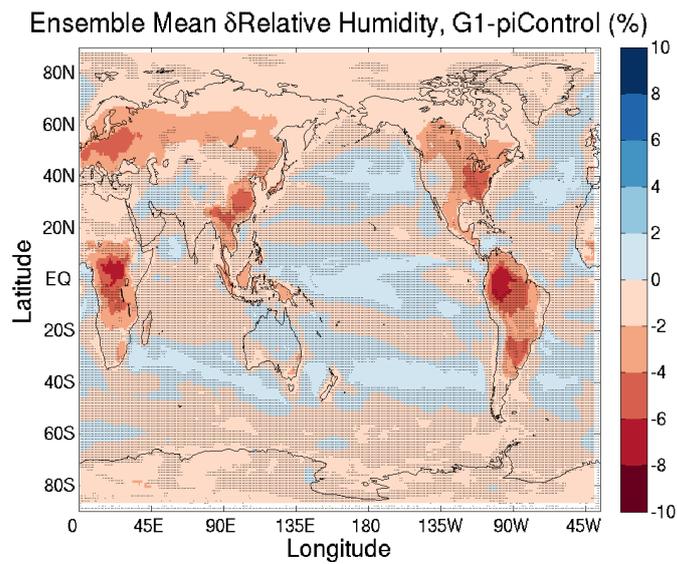
Figure 5. The annual mean near-surface relative humidity anomaly between G1 (years 11-50) and piControl (all years) in eight GCMs. Stippling indicates that fewer than 62.5% of the models agree on the sign of the change. (Data unavailable for HadC, CESM, and MPI models; EC-Earth excluded).
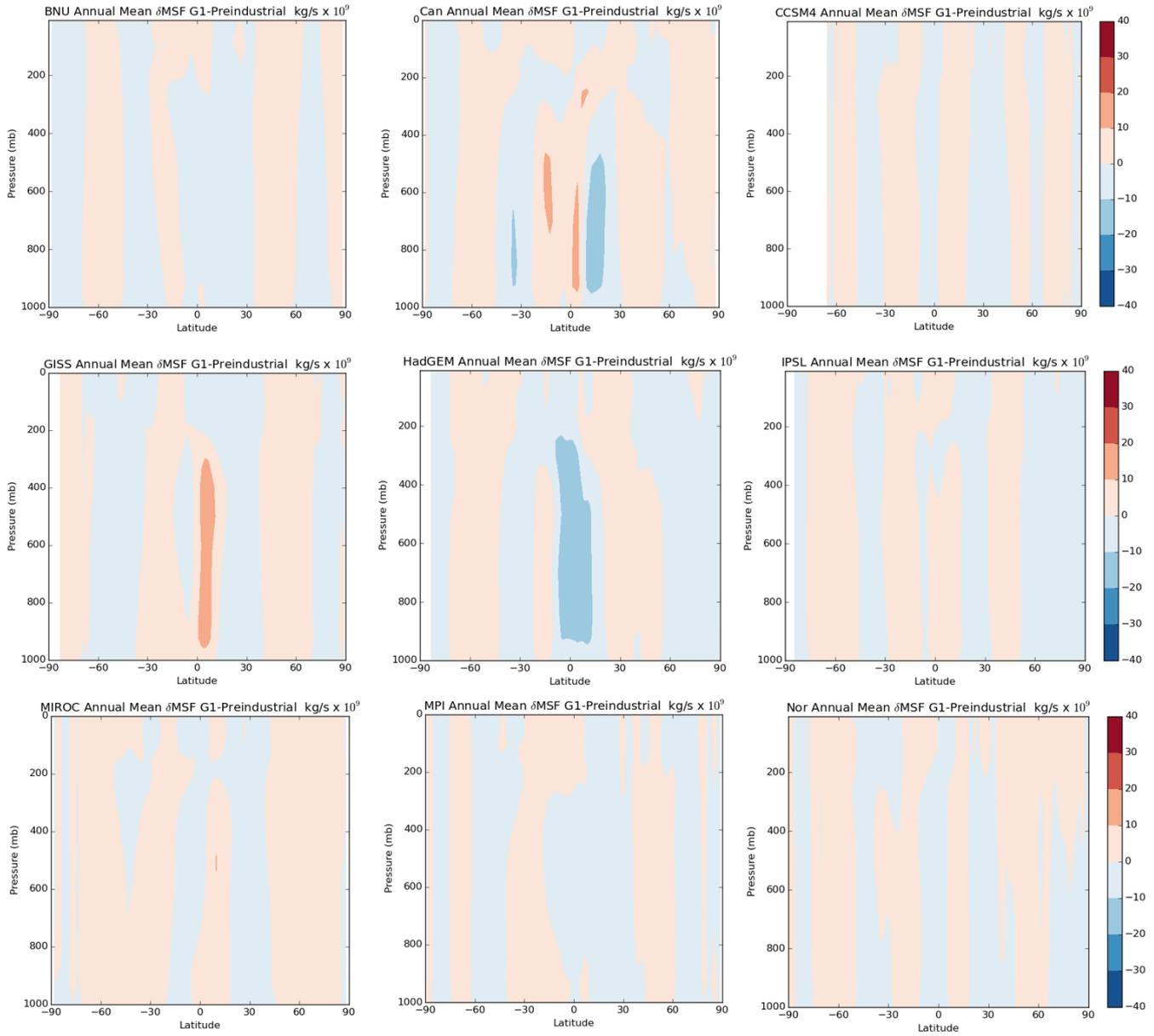
Figure 6. The annual mean meridional streamfunction anomaly between G1 (years 11-50) and piControl (last 40 years) in each model, as calculated in Eq. (4). Blue colors indicate counterclockwise motion. (Data unavailable for HadC and CESM models).
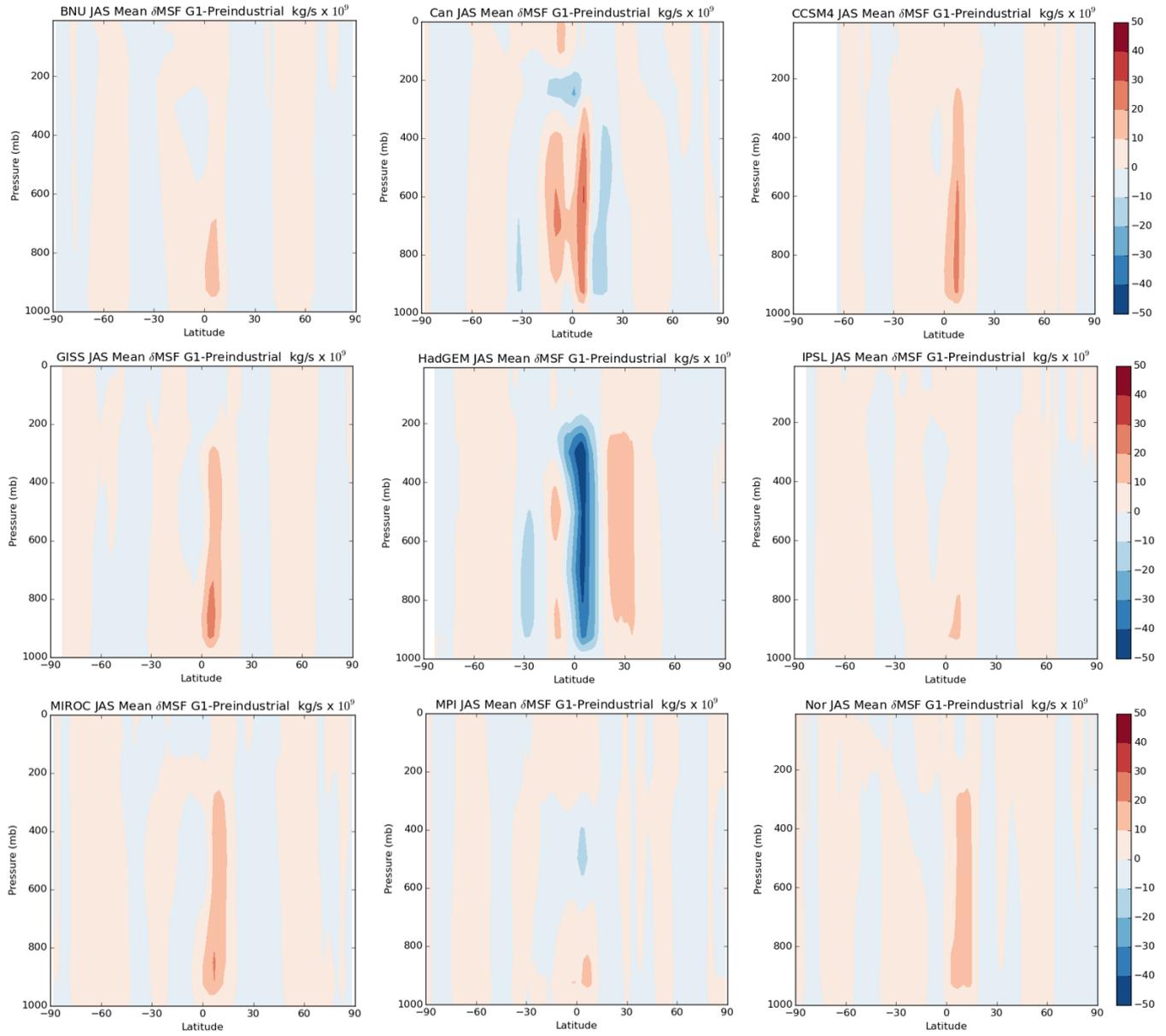
Figure 7. The JAS mean meridional streamfunction anomaly between G1 (years 11-50) and piControl (last 40 years) in each model, as calculated in Eq. (4). Blue colors indicate counterclockwise motion. (Data unavailable for HadC and CESM models).
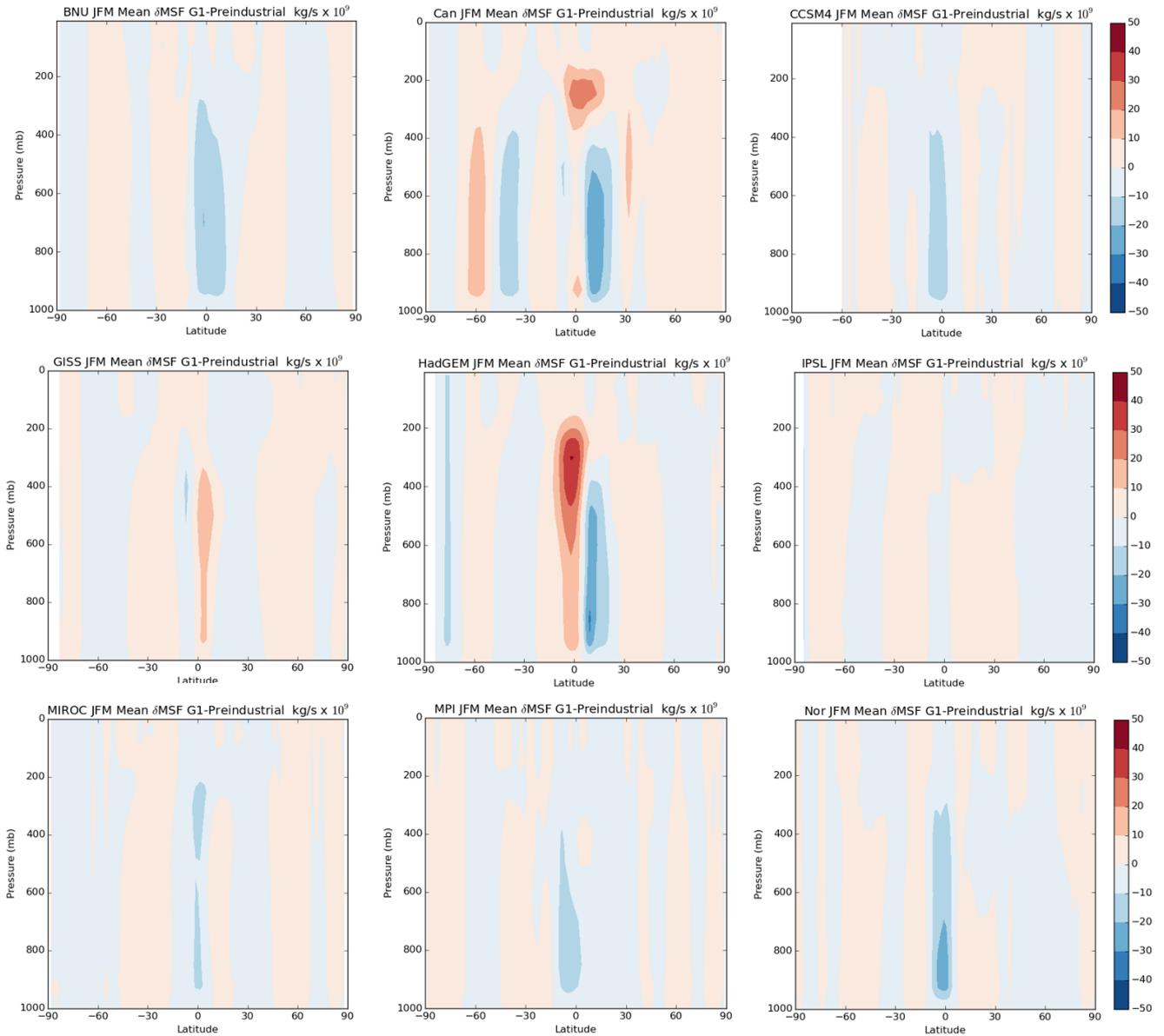
Figure 8. The JFM mean meridional streamfunction anomaly between G1 (years 11-50) and piControl (last 40 years) in each model, as calculated in Eq. (4). Blue colors indicate counterclockwise motion. (Data unavailable for HadC and CESM models).
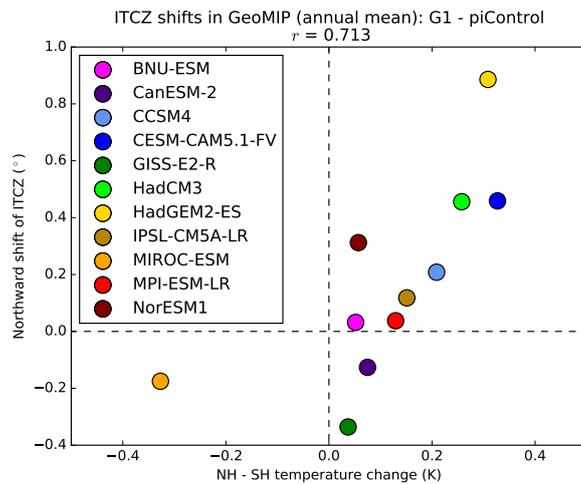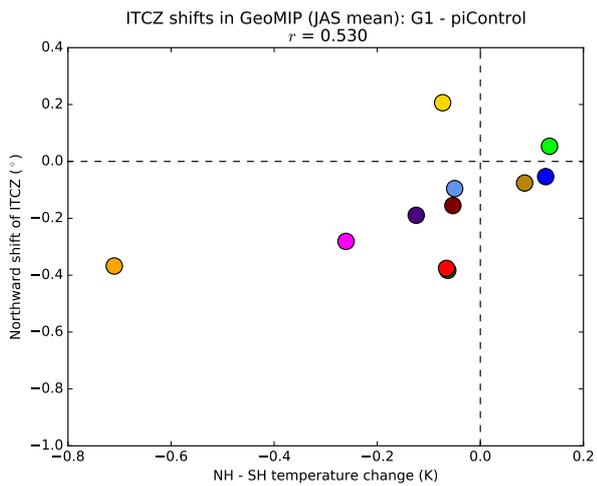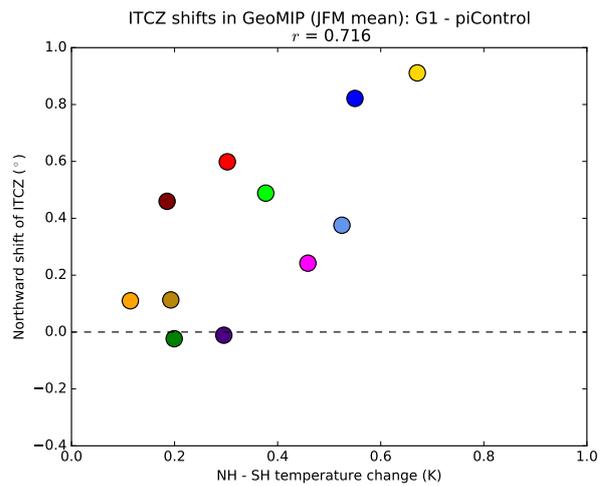
Figure 9. The ITCZ shift vs. the anomaly of the interhemispheric temperature contrast between G1 (years 11-50) and piControl (years 1-40), where r is the correlation coefficient. Panel a) shows the annual mean, b) is the JAS mean, and c) is the JFM mean.
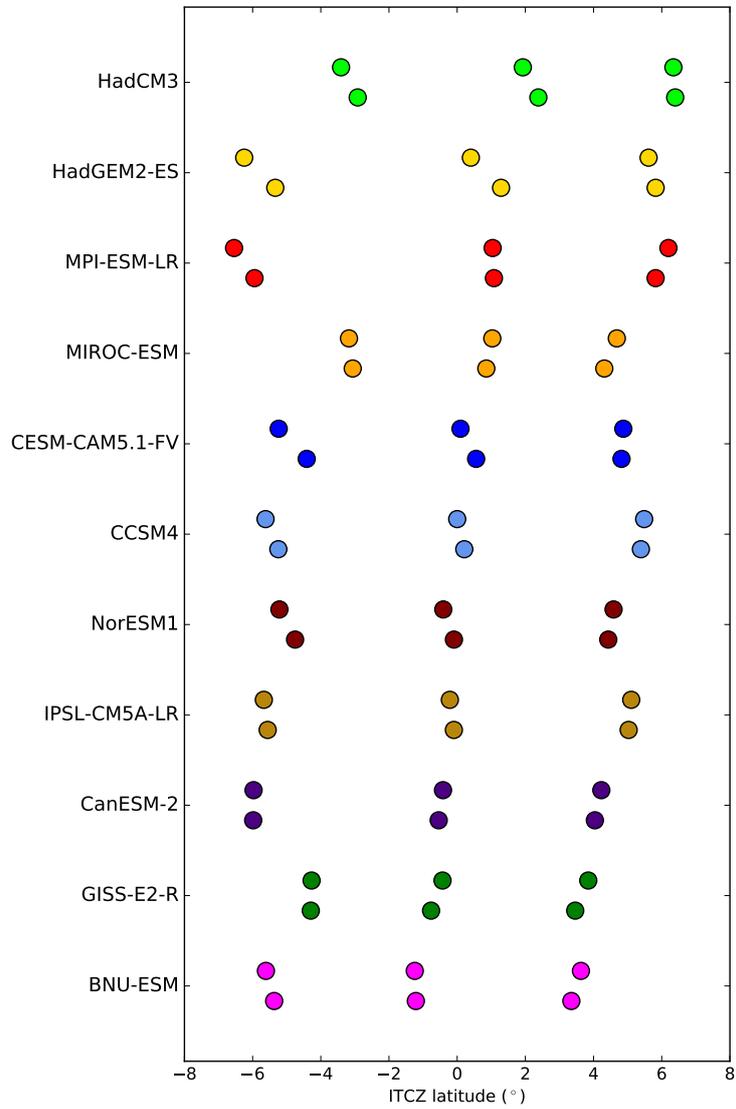
Figure 10. Annual and seasonal mean positions of the ITCZ in piControl (years 1-40) and G1 (years 11-50). For each model, the top row of dots shows piControl positions, and the bottom row of dots shows G1 positions. In each row of dots, the left dot shows the JFM mean position, the middle dot shows the annual mean position, and the right dot shows the JAS mean position. Models are ordered by the annual mean ITCZ position in piControl.

Table 1. GeoMIP Model Specifications. In certain figures models are labeled with the shortened name in parenthesis. Column 3 refers to the CO_2 physiological effect in plants. The solar constant (S_0) reduction is a percentage. Information courtesy of Kravitz et al. (2013a)

Model[1]	Dynamic Vegetation	Phys. Effect	S_0 Reduction	References
BNU-ESM (BNU)	no	yes	3.8	Ji et al. (2014)
Can-ESM2 (Can)	yes	yes	4.0	Arora et al. (2011)
CCSM4 (CCSM4)	no	yes	4.1	Gent et al. (2011)
CESM-CAM5.1-FV (CESM)	no	yes	4.7	Hurrell et al. (2013)
EC-Earth	no	no	4.3	Hazeleger et al. (2012)
GISS-E2-R (GISS)	no	yes	4.5	Schmidt et al. (2014)
HadCM3 (HadC)	no	yes	4.1	Gordon et al. (2000)
HadGEM2-ES (Had)	yes	yes	3.9	Collins et al. (2011)
IPSL-CM5A-LR (IPSL)	yes	yes	3.5	Dufresne et al. (2013)
MIROC-ESM (MIROC)	yes	yes	5.0	Watanabe et al. (2011)
MPI-ESM-LR (MPI)	no	yes	4.7	Giorgetta et al. (2013)
NorESM1-M (Nor)	no	yes	4.0	Bentsen et al. (2013)

1. Full Names: BNU-ESM, Beijing Normal University-Earth System Model; CanESM2, The Second Generation Canadian Earth System Model; CESM-CAM5.1, The Community Climate System Model Version 5.1; CCSM4, The Community Climate System Model Version 4; EC-EARTH DMI, European Earth System Model based on ECMWF Models (Seasonal Forecast System), Danish Meteorological Institute; GISS-E2-R, Goddard Institute for Space Studies ModelE version 2; HadCM3, Hadley Centre coupled model 3; IPSL-CM5A-LR, Institut Pierre Simon Laplace ESM; MIROC-ESM, Model for Interdisciplinary Research on Climate-Earth System Model; MPI-ESM-LR, Max Planck Institute ESM; NorESM1-M, Norwegian ESM.